Vienna Congress on Recent Advances in
Earthquake Engineering and Structural Dynamics 2013 (VEESD 2013)
C. Adam, R. Heuer, W. Lenhardt & C. Schranz (eds)
28-30 August 2013, Vienna, Austria
Paper No. 273

Developing cyclic loading protocols for regions of low to moderate seismicity

P.E.Mergos[1], K.Beyer[1]

[1]Earthquake Engineering and Structural Dynamics Laboratory (EESD), School of Architecture, Civil and Environmental Engineering (ENAC), École Polytechnique Fédérale de Lausanne (EPFL), Switzerland

Abstract. This paper deals with the development of loading protocols appropriate for cyclic testing in regions of low to moderate seismicity in Europe. To serve this goal, cumulative damage demands imposed by a set of 60 ground motion records, representative of a European moderate seismicity region for the 2% probability of exceedance in 50 years seismic hazard level, on a wide variety of SDOF systems are evaluated. To meet the calculated cumulative damage demands, several loading protocols are developed for different structural types, vibration periods and level of reliability (medians or 84[th] percentiles). Protocol comparisons reveal that the proposed loading protocols for the median estimates of cycle amplitudes are significantly less demanding than existing protocols. Consequently, they can result in more cost-effective structural configurations in European regions of low to moderate seismicity.

Keywords: Quasi-static; Loading protocols; Low to moderate seismicity; Cumulative damage

1 INTRODUCTION

Performance based earthquake design requires reliable knowledge of structural members' strength and deformation capacities. In many cases, these capacities cannot be predicted accurately by analytical modelling and experimental testing is required. To do so, quasi-static cyclic tests are typically conducted, which apply predefined displacement histories, named loading protocols, at low velocity rates to structural members or subsystems. In earthquake engineering, however, strength and especially deformation capacities of structures depend not only on structural configuration, but also on the imposed cumulative damage demand (Krawinkler *et al*. 2001). Hence, in order to yield realistic capacity estimates, appropriate loading protocols should reflect the estimated cumulative seismic demands in the regions of interest.

Several loading protocols have been developed in the literature for different types of structural and non-structural components. The list includes but is not limited to: SPD protocol (Porter 1987), CUREE protocols (Krawinkler *et al*. 2001), FEMA-461 protocols (FEMA 2007) and ISO protocol (ISO 2010).All of these protocols have been developed for regions of high seismicity. However, large magnitude earthquakes typically impose higher cumulative damage demands (Kramer 1996). Hence, existing loading protocols may overestimate seismic demand in regions of low to moderate seismicity yielding over-conservative capacity estimates and leading to uneconomic or even not feasible structural designs.

In this study, quasi-static loading protocols will be developed representative of the seismic demand in low to moderate seismicity regions. It is envisaged that the proposed protocols will be applicable to a wide range of structural systems covering a large part of the building stock in these regions. The new protocols are designed in order to address the EC8 performance objectives criteria.

2 DEVELOPMENT OF LOADING PROTOCOLS

2.1 Selection and scaling of ground motions

The main objective of quasi-static cyclic testing is the determination of strength and deformation capacities of structures. The Part-3 of Eurocode 8 (EC8-3) defines deformation capacities Δ_{NC} at the "near collapse" (NC) performance level as the deformations related to a 20% drop of the maximum resistance. Deformation capacities Δ_{SD} for the "significant damage" (SD) performance level are then determined as a fraction of Δ_{NC} (e.g. 75% in EC8-3). Hence, in order to calculate deformation capacities for both limit states, Δ_{NC} should be reliably established.

In order to yield realistic estimates of structural capacities, loading protocols should impose cumulative damage demands similar to the ones anticipated by real earthquakes. Consistently, protocol development should be based on ground motion record sets representative of the seismicity of the region of interest and of the level of seismic hazard.

Following these observations, 60 ground motion records representative of European low to moderate seismicity regions for the 2/50 seismic hazard level are selected. The city of Sion in Switzerland is used herein as the region of reference. The ground motion records sets are chosen in accordance with the de-aggregation of seismic hazard results for this city and the 2/50 seismic hazard level (Giardini *et al*. 2004).In addition to the 60 ground motion records representative of low to moderate seismicity regions, the 20 ground motion records employed in previous studies for developing several loading protocols (e.g. Krawinkler *et al*. 2001, FEMA-461) in high seismicity regions are also examined in the following of this study for comparison reasons.

The selected ground motion records are scaled in order to match the spectral acceleration of the horizontal elastic spectrum of EC8 for the 2/50 seismic hazard level at the vibration period of the structure as suggested by Krawinkler *et al*. (2001). The target EC8 elastic spectrum is derived for soil class C. The peak ground acceleration for the 2/50 seismic hazard level is calculated by multiplying the peak ground acceleration for the 10/50 hazard level by the importance factor γ_I defined by the following equation of EC8-1.

$$\gamma_I = \left(\frac{P_L}{P_{LR}} \right)^{-1/3} = 1.71 \tag{1}$$

In this equation, P_L is the target probability of exceedance in 50 years (2%) and P_{LR} is the reference probability of exceedance in 50 years (10%). The peak ground acceleration for the 10/50 seismic hazard level and the site of Sion is taken equal to 0.16g (SIA 2003), while for the high seismicity earthquakes it is taken equal to 0.40g.

2.2 Selection of representative structural systems

Cumulative damage effects imposed by ground motions are strongly dependent on the type of the structural system. Hence, representative structural systems of those that will be tested need to be examined for the development of loading protocols. In this study, the following structural systems are examined: infinitely elastic, timber walls, reinforced concrete (RC) frames, reinforced concrete and masonry shear walls and rocking masonry walls.

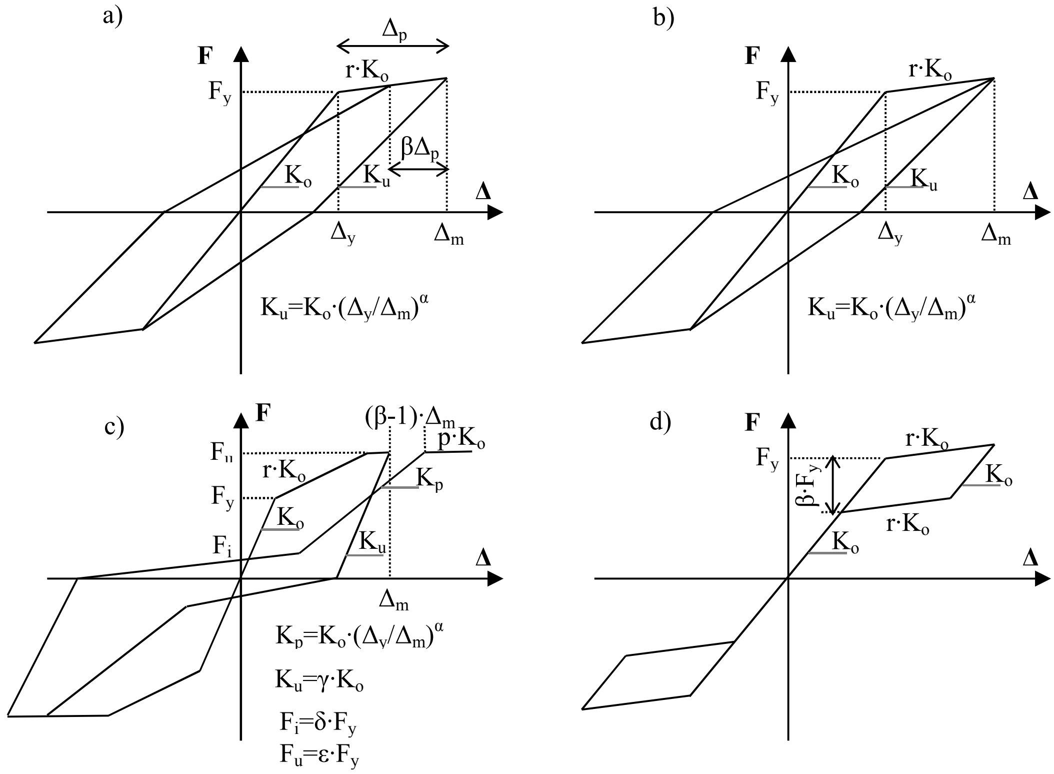

Figure 1: Implemented hysteretic models: a) 'Fat' Takeda (α=0.3, β=0.6); b) 'Thin' Takeda (α=0.5); c) Wayne Stewart (α=0.38, β=1.09, γ=1.45, δ=0.25, ε=1.5, p=0); d) Flag-Shaped (β=0.10)

Table 1. Characteristics of representative structural systems

Structural system	Hysteretic model	Period (sec)	Hardening ratio	q-factors
Infinitely elastic	Elastic (EL)	0.10, 0.20, 0.30, 0.50, 0.75, 1.00, 1.50	-	
Timber walls	Wayne Stewart (WS)	0.10, 0.20, 0.30, 0.50, 0.75, 1.00, 1.50	0.001, 0.01, 0.10, 0.40	1.0, 2.0, 3.0, 4.0, 5.0
RC frames	'Fat' Takeda (FT)	0.15, 0.30, 0.50, 0.75, 1.00, 1.25, 1.50	0.001, 0.01, 0.05, 0.10	1.0, 2.0, 3.0, 4.5, 6.0
RC & masonry shear walls	'Thin' Takeda (TT)	0.10, 0.20, 0.30, 0.50, 0.75, 1.00, 1.50*	0.001, 0.01, 0.05, 0.10	1.0, 2.0, 3.0, 4.5, 6.0*
Masonry rocking walls	Flag shaped (FS)	0.10, 0.20, 0.30, 0.50, 0.75, 1.00, 1.50	0.001, 0.005, 0.01, 0.05	1.0, 1.5, 2.0, 2.5, 3.0

* For masonry shear walls only q-factor values of 1,2 and 3 and vibration periods up to 0.5s are examined

SDOF systems are employed to model structural response. In order for a SDOF system to be representative of a structural system, an appropriate force-displacement hysteretic model has to be selected (Figure 1). Table 2 summarizes the structural systems and the corresponding hysteretic models employed in this study. Following the suggestions by Priestley et al. (2007), the 'Fat' Takeda hysteretic model is applied for reinforced concrete frames and the 'Thin' Takeda for reinforced concrete and masonry shear walls. The Wayne Stewart hysteretic model is adopted for timber walls with the hysteretic parameter values proposed by Stewart (1987) for plywood sheathed timber walls. For rocking masonry walls, the Flag-Shaped hysteretic model is applied. The elastic model is used for all structural systems expected to respond in the elastic regime even for the 2/50 seismic hazard level.

Table 1 also summarises the assumed periods of vibration T and hardening ratios r (ratio of post-yield over elastic stiffness) of the SDOF systems. These values have been selected in order to cover the characteristics of a large percentage of structural systems forming the European building stock.

2.3 Calculation of seismic demands

Linear and nonlinear time history analyses were carried out with computer software RUAUMOKO (Carr 2012), using the Newmark constant average acceleration integration algorithm. The analysis time step used was 0.001s. Tangent stiffness proportional damping was applied since this is considered as a more realistic assumption for inelastic systems (Priestley and Grant 2005). In total, 567 (SDOFs) X 80 (ground motions) =45360 time history analyses were conducted.

It is known that cumulative seismic damage effects are a function of the number, ranges, means and sequence of the imposed deformation cycles (Krawinkler *et al*. 2001). To determine the first three parameters, all displacement responses obtained by the time history analyses of SDOF systems are re-arranged in cycles using the simple rainflow cycle counting algorithm by Downing and Socie (1982). This method identifies cycles as closed hysteretic loops and provides their ranges (difference between maximum and minimum peak) and means (average value of minimum and maximum peak).

The cycle ranges are then centred with respect to zero and they are normalized with respect to the maximum cycle range. This action follows the assumption that the cycle means are negligible and displacement amplitudes are close to the half of cycle ranges (FEMA-461 2007). This assumption is adequately justified by the analytical results obtained in this study as it will be shown in the following. At the end, normalized cycle ranges are placed in descending order. It is important to note that only pre-peak excursions are counted herein since they are the ones causing the most significant structural damage (Krawinkler *et al*. 2001, FEMA-461 2007). Pre-peak excursions are the cycles occurring before the latest of the maximum or minimum displacement response.

For each SDOF system and for the 60 ground motion records for the low to moderate seismicity or the 20 ground motion records for the high seismicity case, statistical measures (medians and 84th percentiles) for each normalized cycle amplitude are calculated (FEMA-461 2007).

As an example, Figure 2a presents the medians of normalized cycle amplitudes for a timber wall SDOF system with vibration period T=0.20s, hardening ratio r=1%, q-factor=1 and for the low to moderate seismicity records. Only damaging cycles are shown. Damaging cycles are considered herein as the cycles with amplitudes greater than 5% of the maximum cycle amplitude (Krawinkler *et al*. 2001).

Figure2b presents some additional information regarding the amplitude sequence of the same SDOF system and seismicity level. In particular, it presents a comparison of the median and 84th percentiles values of the ordered normalized cycle amplitudes. It can be seen that the 84th percentiles are significantly higher than the median values. As a result, the 84th percentiles of 26 normalized amplitudes are greater than 0.05, while only 15 median values are above this limit. This shows the significant scatter of the analytical results for the different ground motion records.

Furthermore, Figure 2b illustrates the median values of the cycle means normalized with respect to the maximum cycle amplitude. It is evident that they remain constantly close to zero (maximum value is 0.12). Hence, mean effects (i.e. asymmetric cycles) can be ignored with reasonable accuracy when developing loading protocols for regions of low to moderate seismicity.

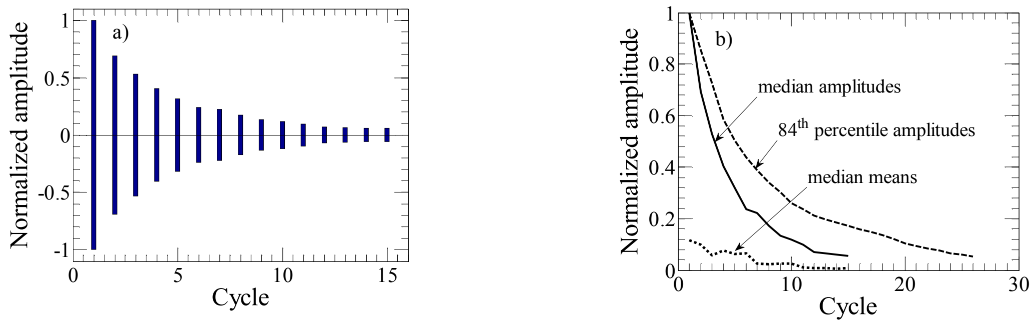

Figure 2: Statistical measures of ordered normalized cycle amplitudes: a) median amplitudes; b) median amplitudes, 84th percentile amplitudes and normalized median means

2.4 Parametric analyses of SDOF systems

In this section, parametric analyses are conducted in order to determine the most critical SDOF systems in terms of cumulative seismic demands. The cumulative damage demand parameter examined herein is the sum of normalized cycle amplitudes $\Sigma\delta_i$, where $\delta_i=\Delta_i/\Delta_{max}$ and Δ_i is the displacement amplitude of cycle i and Δ_{max} is the maximum displacement amplitude of all cycles. In this section, cumulative demand parameters are calculated by the median normalized amplitude sequences (see Figure2a) using the methodology described in the previous section for the low to moderate seismicity records.

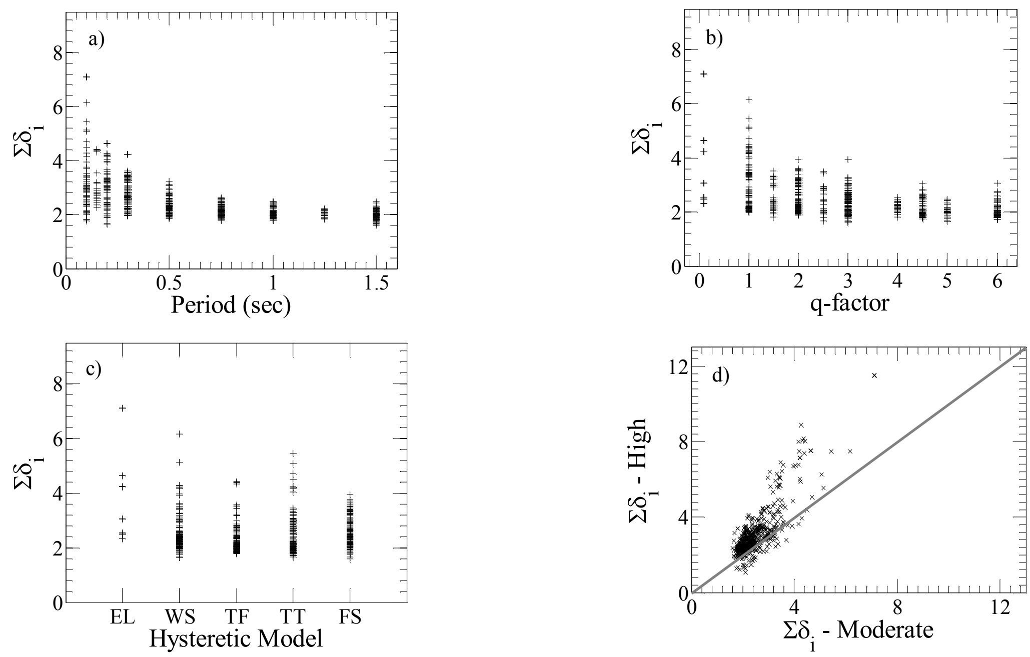

Figure 3: Variation of the sum of normalized displacements $\Sigma\delta_i$ of the median amplitude sequences with: a) vibration periods; b) q-factors; c) hysteretic model for the low to moderate seismicity earthquakes and d) comparison of $\Sigma\delta_i$ demands for the low to moderate vs. high seismicity earthquakes

Figure 3a shows the variation of $\Sigma\delta_i$ with the vibration period. It can be seen that for small periods (less than 0.5s) the cumulative damage demands decrease rapidly with period. However, for higher periods, the rate of reduction with period decreases.

Similarly, Figure 3b presents the variation of $\Sigma\delta_i$ with the applied q-factor. In this figure, the values of the infinitely elastic SDOFs are also presented assuming q-factors close to zero. It can be seen that the elastic systems have the greatest cumulative seismic demands followed by the systems with q-factors equal to unity. For q-factors between 1 and 3, cumulative demands drop rapidly, while for high q-factors (>3) they tend to stabilize.

Figure 3c compares the $\Sigma\delta_i$ values as derived by the application of the different hysteretic models. It can be seen that the elastic system develops the highest cumulative demands followed by the Wayne Stewart, 'Thin' Takeda and 'Fat' Takeda hysteretic models in descending order. The Flag Shaped hysteretic model develops the minimum cumulative seismic demands.

Figure 3d compares the SDOF systems' cumulative demands as derived from the 60 low to moderate seismicity ground motion records and the 20 high seismicity records respectively. It can be inferred that for the vast majority of the SDOF systems, the high seismicity records impose higher cumulative demands than records representing low to moderate seismicity. It is recalled that Figure 3d refers to the sum of normalized cycle amplitudes with respect to Δ_{max}. Comparison of the sum of the absolute displacements $\Sigma\Delta_i$ would naturally be much more severe for the high seismicity records. More importantly, higher seismicity records are significantly more demanding for the SDOF systems with significant cumulative demands that will govern the construction of the loading protocols as it will be explained in the following.

2.5 Construction of loading protocols

In this section, the development of the proposed loading protocols is described. First, the methodology for constructing loading protocols to meet cumulative seismic demands of a specific SDOF system is outlined. Next, the proposed loading protocols corresponding to the critical SDOF systems are presented.

In general, the protocol consists of n load steps with n_1 cycles of the same amplitude per step. Hence, $n_{tot}=n\cdot n_1$ cycles in total. At the beginning, the number of cycles per step is decided. In this study, two cycles per step will be employed for constructing the loading protocols. This is considered as a good compromise as it allows to assess the loss of stiffness and strength between cycles one and two without applying a large number of cycles.

Next, the SDOF's system normalized amplitude sequence is obtained (median values or 84th percentiles) and the corresponding empirical cumulative distribution function (CDF) is constructed. The latter reflects the distribution of the normalized cycle amplitudes. Additionally, the cumulative damage effect (CDE) of the SDOF system cycle sequence is calculated. The basis for calculating the CDE is the following general damage model (Krawinkler *et al*. 2000, Richards and Uang 2006).

$$CDE = C \cdot \sum_{i=1}^{N} \left(\Delta_i\right)^c = C \cdot \left(\Delta_{\max}\right)^c \cdot \sum_{i=1}^{N} \left(\delta_i\right)^c \qquad (2)$$

whereN is the total number of damaging cycles of the SDOF normalized cycle displacement amplitude sequence, C and c are structural performance parameters and the other symbols have already been defined in the previous sections. The parameter c is typically greater than 1 reflecting the fact that larger cycles cause more significant damage (Richards and Uang 2006).

The methodology proposed herein for constructing the loading protocols aims at maintaining a conservative distribution of normalized cycle amplitudes of the SDOF system as well as a conservative total CDE. To achieve this goal, a while-loop is launched, where the number of total steps n progressively increases, cycle amplitudes are then determined to match the SDOF's CDF (see Fig. 9a) and the protocol's CDE is calculated for each new value of n. The loop ends when the protocol's CDE exceeds for first time SDOF's CDE. For the CDE, it is assumed that the structural parameter c is equal to 1. If the protocol's CDE exceeds SDOF's CDE for c=1, then the same holds for all values of c>1. Hence, c=1 may be considered as a conservative assumption.

The afore-described methodology yields arbitrary loading protocol cycle amplitudes and may end up to abrupt amplitude changes between two subsequent load steps ('rough' loading protocol). In order to smooth the loading protocol curve, the following general exponential function is proposed in this study

$$f(x) = -0.50 + 0.55 \cdot \exp\left[\left(\frac{x}{n}\right)^{a}\right] \tag{3}$$

where x is the current load step, n is the number of total steps of the 'rough' protocol and α is a parameter determining the rate of amplitudes increase. Equation (3) satisfies the basic boundary conditions (i.e. f(0)=0.05 and f(n)=1). Furthermore, it requires only two parameters (i.e. n and α) for fully determining the loading protocol sequence. Hence, it is useful also for standardization reasons, when more than one protocol is developed, as it is the case in this study.

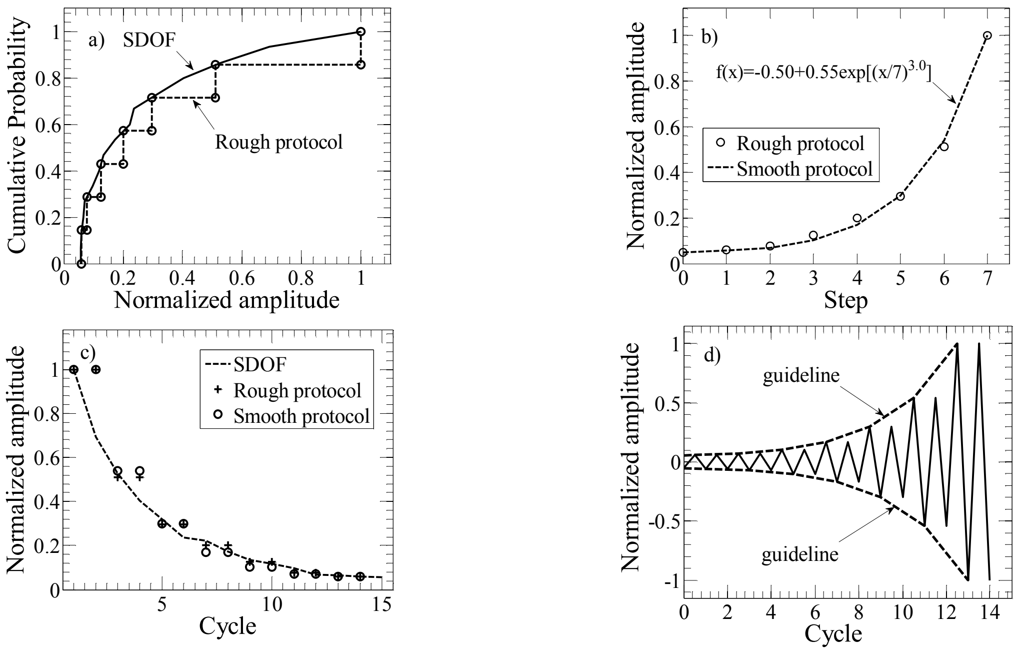

Figure 4: Loading protocol construction: a) comparison of loading protocol and SDOF normalized cycle amplitude CDFs; b) comparison of rough and smooth protocol normalized amplitudes; c) normalized cycle amplitude sequences of the SDOF system the rough and the smooth protocol and d) derived loading protocol

Figure 4 presents loading protocol development for the median amplitude sequence of the SDOF system described in section §2.3 (Figure2a). Figure4a presents the comparison of the empirical normalized cycle amplitude CDFs of the SDOF system and the derived protocol. The loading protocol CDF meets SDOF's CDF at the end of each load step (every two cycles). In this manner, the loading protocol's CDF approaches and remains always below the SDOF's CDF. This is on the conservative side since it indicates that the protocol has a higher percentage of large cycle amplitudes.

Figure4b compares the predictions of Eq. (3) for n=7 and α=3.0 with the normalized amplitudes of the 'rough' protocol for the SDOF system under examination. Very good convergence is achieved. Furthermore, Figure4c compares the normalized amplitudes of the SDOF system, the 'rough' and the 'smooth' protocol. The protocols follow closely SDOF's response, yet remaining conservative for the large cycle amplitudes. Finally, Figure4d illustrates the derived 'smooth' loading protocol. It consists of 7 load steps of 2 equal cycles each yielding 14 cycles in total. Load step cycle amplitudes are determined by the two guidelines defined by Eq. (3) for n=7 and α=3.0.

2.6 Proposed loading protocols

In this section, the proposed loading protocols developed for quasi-static cyclic experimental testing of structural components or systems are presented. To avoid over-conservative solutions, different loading protocols are developed herein as a function of seismicity level, vibration period and structural system. For each of these combinations, the most critical SDOF system, in terms of CDE, will be selected from all combinations of q-factors and hardening ratios. The loading protocols will be developed for both median and 84th percentile estimates of normalized cycle amplitudes (see Figure 2b). In all cases, the proposed loading protocols are expressed as a fraction of the maximum displacement demand Δ_{max}.

Table 2 summarizes the resulting smooth protocol parameters (n and α) derived from the critical SDOF systems representative of different structural configurations and levels of seismicity. It is recalled that n is the total number of load steps. Since two cycles per step are assigned, the total number of cycles n_{tot} is always equal to 2n. It can be seen that protocol parameters vary significantly with the structural type, level of seismicity (low to moderate vs. high) and level of reliability (medians vs. 84th percentiles). The next section presents a more comprehensive comparison of the proposed loading protocols.

Table 2. Proposed protocol parameters for different structural systems and levels of seismicity

Structural system-Hysteretic model	T (sec)	Moderate-low seismicity		High seismicity	
		Medians	84th percentiles	Medians	84th percentiles
Infinitely elastic-Elastic (EL)	T=0.1s	n=12 α=3.05	n=23 α=2.65	n=22 α=3.22	n=74 α=5.03
	T=0.2s	n=6 α=2.00	n=17 α=2.65	n=12 α=2.44	n=24 α=2.34
	T=0.3s	n=5 α=1.45	n=11 α=1.73	n=12 α=2.49	n=18 α=2.13
	T≥0.5s	n=3 α=1.56	n=11 α=2.56	n=5 α=1.98	n=17 α=3.38
Timber walls-Wayne Stewart (WS)	T=0.1s	n=12 α=3.97	n=22 α=3.77	n=15 α=3.58	n=49 α=5.74
	T=0.2s	n=7 α=2.93	n=16 α=3.70	n=16 α=3.21	n=32 α=3.49
	T=0.3s	n=6 α=2.98	n=13 α=3.08	n=11 α=2.4	n=23 α=2.79
	T≥0.5s	n=5 α=3.07	n=13 α=3.95	n=6 α=2.75	n=16 α=3.08
RC frames-Fat Takeda (FT)	T=0.15s	n=7 α=3.3	n=15 α=2.57	n=14 α=2.80	n=43 α=3.81
	T=0.3s	n=5 α=1.96	n=10 α=2.3	n=10 α=1.94	n=24 α=2.79
	T≥0.5s	n=2 α=1.66	n=8 α=2.6	n=5 α=2.40	n=15 α=3.15
RC & masonry shear walls-Thin Takeda (TT)	T=0.1s	n=11 α=4.17	n=18 α=3.11	n=16 α=4.19	n=36 α=4.59

	T=0.2s	n=6 α=2.26	n=14 α=2.78	n=11 α=2.66	n=33 α=3.91
	T=0.3s	n=5 α=2.16	n=14 α=3.4	n=10 α=2.28	n=22 α=2.99
	T≥0.5s	n=3 α=1.63	n=9 α=1.94	n=6 α=2.27	n=14 α=2.82
Masonry rocking walls-Flag-shaped (FS)	T=0.1s	n=4 α=1.21	n=11 α=2.31	n=7 α=2.25	n=29 α=4.20
	T=0.2s	n=5 α=2.25	n=10 α=1.96	n=7 α=2.96	n=24 α=3.67
	T=0.3s	n=4 α=1.83	n=10 α=2.27	n=8 α=2.86	n=16 α=3.08
	T≥0.5s	n=3 α=1.63	n=11 α=2.87	n=5 α=2.03	n=12 α=3.16

3 COMPARISON OF LOADING PROTOCOLS

In this section, the proposed loading protocols for the different structural systems, levels of seismicity and reliability are compared. In addition, the proposed protocols are compared with three well established loading protocols in experimental testing: the CUREE loading protocol developed for wood-framed shear wall structures and ordinary ground motions (Krawinkler *et al*. 2001), the FEMA-461 displacement controlled loading protocol for drift sensitive non-structural components (FEMA, 2007) and the ISO (ISO 2010) loading protocol for timber shear wall structures. All these protocols have been developed as a function of maximum displacement. Hence, a general comparison with the proposed protocols is possible.

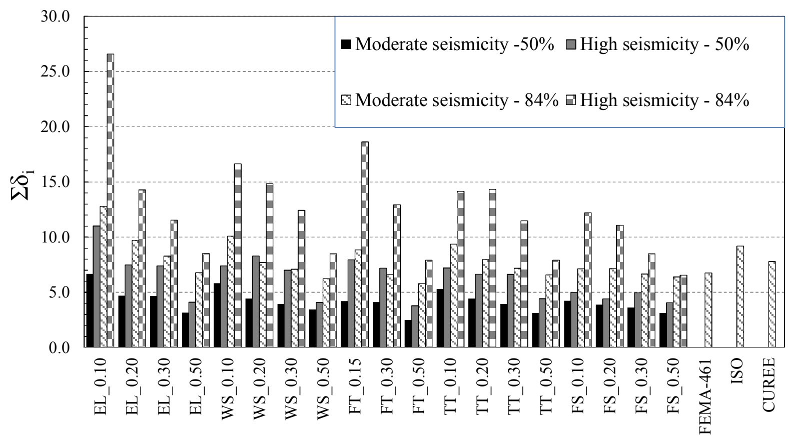

Figure5: Comparison of proposed and existing loading protocols in terms of $\Sigma\delta_i$

Figure 5 compares new and existing loading protocols in terms of the sums of normalized displacements $\Sigma\delta_i$. This cumulative damage parameter is chose herein because it contains information on both the number and the amplitude distribution of loading protocols' imposed cycles. In this figure, structural systems are depicted with two letters followed by a number. The two letters are the abbreviations of the hysteretic model (see Table 1) and the number expresses the vibration period in seconds.

Figure 5 shows that low to moderate seismicity protocols impose always significantly lower cumulative seismic demands than high seismicity protocols. Hence, application of high seismicity protocols in regions of low to moderate seismicity overestimates cumulative damage demands.

Comparison of the existing with the new protocols reveals further that, in general, existing protocols impose similar cumulative demands to the proposed protocols derived for high seismicity and median cycle amplitude estimates. On the other hand, proposed protocols for regions of low to moderate seismicity, as derived for median cycle amplitudes, are importantly less demanding than existing protocols. Hence, their application may lead to less conservative estimations of structural capacities.

4 CONCLUSIONS

Existing loading protocols have been developed for high seismicity regions. In this study, loading protocols are developed for European regions of low to moderate seismicity. The loading protocols are proposed as a function of the structural type, vibration period and level of reliability (medians or 84th percentiles). Comparisons show that the proposed protocols impose significantly smaller cumulative damage demands than existing protocols. Hence, they do not tend to underestimate strength and deformation capacities and the results of these testscan therefore lead to more cost-effective structural configurations.

ACKNOWLEDGEMENTS

Financial support for this research was provided by the Swiss National Science Foundation within project NRP-66 (Resource Wood, Project Nr.406640-136900). The opinions, findings, and conclusions expressed in this paper are those of the authors and do not necessarily reflect those of the sponsoring organization.

REFERENCES

Carr, A.J. (2012). *Ruaumoko – A computer program for inelastic time history analysis*. Department of Civil Engineering, University of Canterbury, New Zealand.

CEN (2005). *Eurocode 8: Design of structures for earthquake resistance.* EN 1998-3, Brussels.

Downing, S.D. and Socie, D.F. (1982). Simple rainflow cycle counting algorithms. *International Journal of Fatique* **4**:31-40.

Gatto, K. and Uang, C. (2003). Effects of loading protocol on the cyclic response of woodframe shearwalls. *Journal of Structural Engineering* **129**:1384-1393.

FEMA-461 (2007). *Interim protocols for determining seismic performance characteristics of structural and non-structural components through laboratory testing*. Federal Emergency Management Agency, Washington.

ISO-21581 (2010). *Timber structures- static and cyclic lateral load test methods for shear walls*. International Standards Organization, Geneva, Switzerland.

Kramer, S.L. (1996). *Geotechnical earthquake engineering.* Prentice Hall, New Jersey.

Krawinkler H., Parisi F., Ibarra L., Ayoub A. and Medina R. (2001). *Development of a testing protocol for woodframe structures*. CUREE publication No.W-02.

Porter M.L. (1987). Sequential phased displacement (SPD) procedure for TCCMAR testing. In: *3rd meeting of the joint technical coordinating committee on masonry research*, US-Japan coordinated program.

Priestley, M.J.N., Calvi, G.M. and Kowalsky, M.J. (2007). *Direct displacement based seismic design of structures.* IUSS Press, Pavia, Italy.

Priestley, M.J.N. and Grant, D.N. (2005). Viscous damping in seismic design and analysis. *Journal of Earthquake Engineering* **9(sup2)**:229-255.

Richards, P.W. and Uang, C. (2006). Testing protocol for short links in eccentrically braced frames. *Journal of Structural Engineering* **132**:1183-1191.

SIA 261 (2003). *Actions on structures*. Swiss Society of Engineers and Architects, Zurich.

Stewart, W.G. (1987). *The seismic design of plywood sheathed shear walls*. PhD Thesis, University of Canterbury, New Zealand.